

Hybrid Time-Base Device for Coherent Sampling Oscilloscope

Tomas Tankeliun¹, Oleg Zaytsev², Vytautas Urbanavicius³

¹ Department of Electronic Systems, Faculty of Electronic, Vilnius Gediminas Technical University, Naugarduko str., No. 41, LT-03227, Vilnius, Lithuania, tomas.tankeliun@vgtu.lt

² Eltesta UAB, Vytenio str. 20, LT-03227, Vilnius, Lithuania

³ Department of Electronic Systems, Faculty of Electronic, Vilnius Gediminas Technical University, Naugarduko str., No. 41, LT-03227, Vilnius, Lithuania

In this paper, a hybrid time-base (HTB) device for the coherent sampling oscilloscope is presented. The HTB device makes it possible to reduce the uncertainty of determining the time position of the sample in the horizontal channel of the sampling oscilloscope. For its functioning, the proposed HTB device requires that the system-under-test, in addition to the test signal, also has a synchronous reference clock – harmonic oscillation. It should be noted that both the test signal and the harmonic reference clock are sampled simultaneously. The harmonic reference clock is connected to one of the oscilloscope channels and a special algorithm processes the clock samples and adjusts the coherent sampling mode. Two techniques of determining the position of the sample on the time axis are combined in the HTB device – the “trigonometric”, when the position is calculated by the arccosine or arcsine formula of the reference clock sampling value, and the interpolation method, according to which the time position of the sample is found by averaging the positions of two adjacent samples, obtained using said “trigonometric” technique. Primary experimental studies have shown that using the HTB device can reduce jitter of the sampling oscilloscope by several times and the drift with constant time distortion components is practically absent in this device.

Keywords: Sampling oscilloscope, jitter, hybrid time-base, coherent sampling, axis of equivalent-time, signal waveform restoration.

1. INTRODUCTION

It is a well-known fact that oscilloscopes are used to observe and measure temporal electrical waveforms and this is confirmed again by Pereira in his revision study [1]. Measuring periodic broadband signals, the sampling oscilloscopes have an undeniable advantage against conventional real-time oscilloscopes – this is a comparatively low price with the same metrological characteristics, as stated in the work by Haley and colleagues [2]. This paper shows that sampling oscilloscopes have bandwidths up to 100 GHz and are available with nominal 50 Ω input impedances; these oscilloscopes are flexible and easy to use. This attractive feature of the sampling oscilloscope is due to their microwave circuits being concentrated in the front-end part of this measuring instrument, while their relatively low-frequency circuits perform the main processing of the measured waveform.

Probably the widest application area of sampling oscilloscopes, where their unique metrological characteristics are used, is in the calibration of broadband instruments and measurement systems. Examples of the study of the diversity of the use of sampling oscilloscopes can be found in the works of Remley, Avolio and their colleagues [3], [4]. From their work it is clear that sampling oscilloscopes are

indispensable tools in the systems of accurate measurement of high-speed electrical waveforms of equipment of the 5G wireless communication and in calibration of nonlinear measurements of the temporal current and voltage waveforms of microwave transistors. Such measuring systems are based on a very fast sampling oscilloscope with electrooptic interactions and have measurement bandwidths of many hundreds of gigahertz. An example of a record of on-wafer measurements of heterojunction bipolar transistors in the frequency band up to 1.1 THz by sampling systems is also given in [3].

Restoration of the waveform of the measured signal in the sampling oscilloscope is performed from the instantaneous values of the signal – samples that are a function of time. Data sheets reported by well-known manufacturers Tektronix, Inc. [5] and Keysight Technologies, Inc. [6] indicate that the sampling value in modern sampling oscilloscopes is most often measured by 16-bit ADCs, which, in the ideal case, make it possible to achieve a negligibly small vertical channel measurement uncertainty not exceeding 0.002 percent. Besides, a significant portion of the voltage errors are reduced by using the built-in DC calibration of the oscilloscope to correct for gain errors, offset errors, and “nonlinear distortion” – the manufacturer’s term for the voltage

distortion that can change at different voltage levels. And also, the nonlinear distortion is corrected within the oscilloscope with an internal lookup table [7]. Samples are fixed once during the period of the measured signal or even less frequently, therefore, in sampling oscilloscopes accurate determination of sampling time is especially important [2]. However, a review of the technical parameters of sampling oscilloscopes by the above manufacturers [5], [6] shows that the jitter (one of the main components of the time-base (TB) measurement errors) of top models can exceed 2 percent with respect to the period corresponding to the limiting frequency of the passband. It is also known that, in addition to jitter, the accuracy of the position of the sample on the time axis is determined by errors due to drift and TB distortions [7]. At the same time, the requirement to measure high-speed data transmission systems forces developers and manufacturers to constantly improve sampling oscilloscopes in order to reduce the measurement time uncertainty.

The time-base device, the accuracy of which is under a lot of research, performs monitoring of the time position of the sample of the measured waveform in the sampling oscilloscope. In general, the accuracy of the TB device depends on the following factors: jitter – random error having statistical distribution laws; time distortions – constant distortions due to the non-linearity of the elements of the TB device; drift distortions – distortions associated with fluctuations in temperature, instability of power sources and so on. A review of available publications shows that the possibilities of increasing the accuracy of measurements with sampling oscilloscopes using various calibration techniques are most often investigated. For example:

High-speed photodiodes and lasers are used by Clement, Remley, Fuser and their colleagues [7], [8], [9] as a reference input pulse source to calibrate the magnitude and phase response of the sampling oscilloscopes to 110 GHz. The impedance of the oscilloscope and the reference photodiode were considered here and used to correct electrical reflections and distortions due to impedance mismatch; TB imperfections such as drift, TB distortion, and jitter have been corrected as well.

A comprehensive method of reducing the error of the TB device for high speed sampling oscilloscope is presented in work [10]. Here, to reduce TB drift, it is recommended to maintain a stable temperature in the laboratory, the oscilloscope needs a one-hour preheating, and all the measurement experiments are required to finish in 15 minutes (seems to be recommended in studies [7], [11]); it is proposed here to use the least squares method to compensate for the nonlinear distortions of the TB device, and to compensate for jitter the so-called mod decomposition method has been chosen.

A periodic any shape test signal is used in work [12] to estimate and compensate for TB distortions. The information obtained from the values of the measured periods of the signal-under-test allows to find the magnitude of the TB distortion and, accordingly, to compensate for it.

An apparatus, based on a passively mode-locked erbium-doped fiber laser that is phase locked to a microwave generator is used for correcting the TB errors of an

equivalent-time sampling oscilloscope in study [13]. It is stated here by Jargon and colleagues that the mentioned equipment allows to simultaneously correct both the random jitter and the systematic TB distortions.

The use of in-phase and quadrature reference signals to calibrate the oscilloscope time base has been studied by many authors [14], [15]. The presence of two synchronous harmonic signals shifted relative to each other by 90 degrees allows using only steep sections of the reference oscillation waveform, thus increasing the accuracy of determining the temporal position of the sample of the signal-under-test.

In the case where the sample position on the time axis is determined from the measured values of the reference signal, the calibration of the vertical channel of the oscilloscope is also important. Cho and colleagues [16] derived the equations of ADC signals in closed form and obtained exact solution for time-interleaved errors. Experimental verification of the proposed method showed that, after this calibration, it was possible to reduce the mismatch of the oscilloscope channels to –100 dBV.

It is also necessary to note that the special procedure for correcting the TB distortion of waveforms measured by an equivalent-time sampling oscilloscope, which is developed by the National Institute of Standards and Technology (NIST) [19], is used in many studies [11], [13], [18], [19].

Studies dedicated to reducing TB uncertainty with circuit design, signal processing or technological approaches are found in open publications much less frequently than calibration techniques. Such a rare example of signal processing research to reduce jitter is the work of Nelson [20], where analog signal processing, implemented as a “three-phase phase-gate track&hold” circuit, coupled with a temperature-compensated high-Q VCO, allows to achieve a typical timing jitter of 8 ps RMS hundreds of microseconds from the trigger position, considering both random and deterministic sources of timing error.

In our paper, the problem of reducing time-base errors is solved by a hybrid approach. It is known that most data transmission systems-under-test have an internal reference clock oscillator [11]. The proposed hybrid TB device uses such an external oscillator, as well as the measuring modules and a special data processing and control algorithm of the sampling oscilloscope itself.

2. HYBRID TIME-BASE ARCHITECTURE

Techniques for determining the time position of the sample, block diagram of device hardware and algorithm for data processing and control make up the architecture of the proposed hybrid time-base.

A. Basic principles

The time position of the sample of the signal-under-test in the proposed hybrid TB device is determined on the basis of the assumption of complete synchronism of the signal and the reference clock (Fig.1.). It should be specially noted that this clock must be harmonic, i.e., it must change in time as a function of the sine or cosine. In general, the synchrony between the signal-under-test and the harmonic reference

clock can be achieved in various ways, for example: a) the system-under-test and the TB device are started by a common external generator of harmonic oscillations, b) the system-under-test has an internal generator of harmonic reference clock, c) the harmonic reference clock is made inside the TB device itself from the signal-under-test using, for example, a low-pass filter. Two techniques for calculating the time position of the sample of the signal-under-test are used in the proposed HTB device: “trigonometric”, and the method of interpolation of “adjacent points”. Switch-over from one technique to another depends on the ratio of the value of the sample and amplitude of the harmonic reference clock.

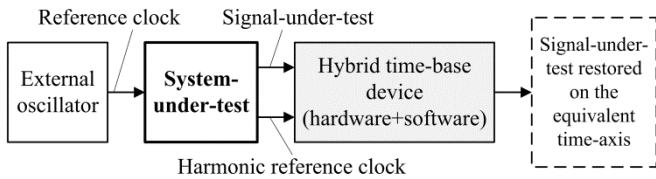


Fig. 1. Hybrid time base architecture.

The “trigonometric” technique involves calculating the time position t_{Tri} of the i^{th} sample by performing an arccosine operation on the value of the reference oscillation sample $y(t_i)$ itself (Fig.2.):

$$t_{Tri} = T \pm \frac{T}{2\pi} \cos^{-1} \frac{y(t_i)}{A}; \quad (1)$$

where “+” corresponds to the falling part of the sinusoid, and “-” corresponds to the rising part of the sinusoid; t_{Tri} is calculated time position; T is the period of the reference clock; A is an amplitude of the reference clock. If the sample of the clock is fetched on a steep part of the sinusoid, then its position will be calculated quite accurately (Fig.2.b).

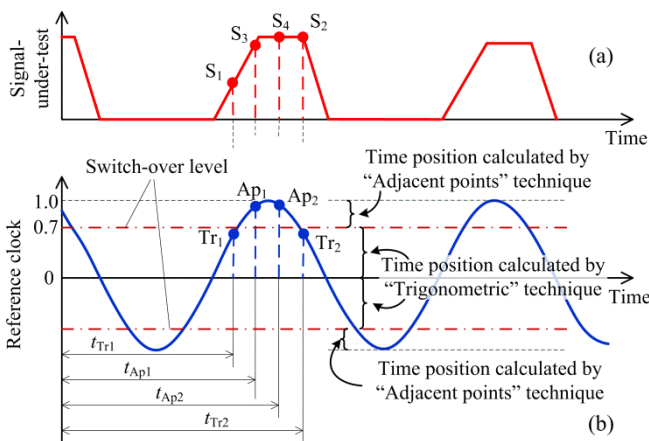


Fig.2. Scheme for determining the time position of samples: where a) is a waveform of the signal-under-test, b) is a waveform of the reference clock.

Otherwise, i.e., when the sample is fetched at the sinusoid top or near the top, because of the amplitude measurement noise, the estimated time position of the sample will be less

accurate. This leads to distortion of the equivalent-time axis in the restoration of the waveform of the signal-under-test.

In order to overcome this drawback, we propose when the moment value of the reference clock approaches its amplitude (about 0.7–1.0 amplitudes), i.e., the sample is fetched on the sloping part of the sinusoid, the calculation of the sample time position is performed in accordance with the “adjacent points” technique. In this case, the interpolation of “adjacent points” technique gives a more accurate result than the “trigonometric” one. Note again that in most cases the “trigonometric” technique allows us to calculate the time position of the sample more accurately and it is inferior to the interpolation of “adjacent points” technique only when the sample is in the sloping part of the sinusoid.

Let us briefly present the essence of the interpolation of the “adjacent points” technique. The time position of the samples fetched in the sloping part of the sinusoid is calculated, taking into account the time position of the two boundary “adjacent” points, calculated by the “trigonometric” technique and they are located on opposite steep slopes of the reference clocks (points Tr_1 and Tr_2 in Fig.2.b)). Samples fetched on the sloping part of the sinusoid are distributed uniformly, interpolating the time interval between these two “adjacent” samples located on steep sections of the sinusoid (points Ap_1 and Ap_2 in Fig.2.b)). The time position t_{Apj} of the i^{th} sample in accordance with the method of “adjacent points” is calculated by the following equation:

$$t_{Apj} = t_{Tri} + \frac{t_{Tri(i-1)} - t_{Tri}}{m+1} j; \quad (2)$$

where t_{Tri} is the last time position in the same half-cycle of the sinusoid, calculated by (1); m is the number of points in one section of the signal image, which is restored by the method of “adjacent points” ($m = 2$ in Fig.2.).

Thus, in the presented new HTB device, when the sample is fetched from the steep portion of the sine wave of the reference clock, the “trigonometric” technique is used, and when the sample is fetched from the sloping portion of the sinusoid that is closer to its top, the interpolation of “adjacent points” technique is applied. To determine the condition for using one or another technique the concept of the “Switch-over level” between the techniques of calculating the time position of the sample is introduced.

B. Organization of the hybrid time-base device hardware

The organization of the new hybrid TB hardware is presented in the block diagram in Fig.3. Its main feature is that the time delays as in the case of sequential sampling [4], are not formed here and the positions of the samples in time are given by means of processing of the harmonic reference clock samples.

Unlike random sampling [4] in our case we need sampling and reference clock synchronicity. The initial stage of measurement in the hybrid TB device is its calibration, i.e., setting the sampling frequency, which corresponds to the coherent mode [21]. This mode in our case is somewhat different from the traditional one [21] and is described below.

Coherent sampling mode condition in the HTB device is defined by the equation:

$$\frac{f_r}{f_s} = M_c + \frac{1}{P}; \quad (3)$$

where f_s is the sampling frequency; f_r is the frequency of the harmonic reference clock, which is synchronous with the signal-under-test; M_c is the integer number of periods of the reference clock for one period of the sampling frequency; P is the number of samples in one period of the reference clock on the axis of equivalent-time of the coherent sampling mode. Since the signal-under-test and the reference clock are synchronous, the sampling frequency is calibrated by a kind of “scanning” relative to the frequency of the reference clock.

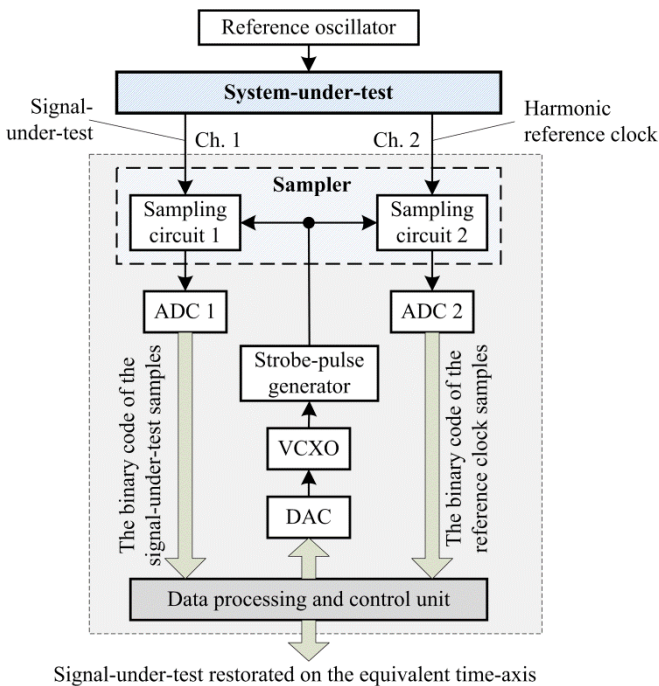


Fig.3. Block diagram of the hybrid time-base device.

The “scanning” is carried out by a sequential change of the code supplied to the digital-to-analog converter (DAC). The output voltage of the DAC changes the frequency of the voltage controlled crystal oscillator (VCXO) which starts the strobe-pulse generator. The samples of the reference clock are then measured, using sampling circuit 2 and the analog-to-digital converter 2 (ADC 2), and processed by the control unit.

The hardware device of the hybrid TB consists of a two-channel sampler, while the strobe pulse that opens the sampling circuits is common (the strobe pulses go to both sampling circuits at the same time). Thus, the time jitter between the strobe pulses of the sampling circuit 1 and sampling circuit 2 will be minimal. The strobe-pulse generator, which generates a common strobe pulse, is triggered from the VCXO, whose frequency can be controlled in small limits, while remaining fairly stable. Frequency

tuning is provided by the DAC controlled by the data processing and control unit.

The signal-under-test and the reference clock must be synchronous, that is, their repetition frequencies should be equal or multiple. In this case, when the signal-under-test is applied to the sampling circuit 1, a strictly harmonic clock, synchronous with the signal-under-test, is fed to the sampling circuit 2. By changing the frequency of the VCXO and analyzing the data obtained from the sampling circuit 2, according to the procedure written below (see the algorithm for time-base data processing and control), control unit establishes a coherent sampling mode with a shift of the strobe-pulses relative to the reference clock for a small part of its period. Thus, the strobe pulses are sequentially shifted relative to the reference clock, ensuring its measurement at several points over the period. In addition, finally, based on the strictly harmonic nature of the reference clock, an axis of equivalent-time is formed at the second sampling circuit. Moreover, since the axis of equivalent-time is common for both sampling circuits, the exact axis of equivalent-time is obtained for the signal-under-test as well.

C. An algorithm of data processing and time-base control

A simplified flowchart showing the procedures for calibrating the TB device, forming the axis of equivalent-time and restoring the waveform of the signal-under-test is shown in Fig.4. There are seven steps in the algorithm.

Let us discuss briefly the step-by-step operation of the algorithm.

Step 1. The samples of the signal-under-test and the harmonic reference clock are accumulated during the main cycle of restoration of the image of the signal-under-test (steps 1, 2, and 5–7) and the sampling frequency calibration cycle (steps 1–4). Two arrays of a fixed identical length N of samples are formed in this case: signal-under-test and clock.

Step 2. The operating mode of the TB device is checked. If the number of samples in one period of the reference clock n does not correspond to the preset one, i.e., the coherent sampling mode is not set up – the main measurement cycle (steps 5–7) is not performed, but instead, the sampling frequency calibration procedure (steps 1–4) is performed. During this procedure, the frequency of the strobe generator (Fig.3.) changes in such a way that condition (2) is fulfilled.

Step 3. The accumulated array of samples of the reference clock is analyzed in this way:

- a) Using the values of the samples accumulated in the reference clock array, the mode evaluation coefficient k is calculated:

$$k = \sum_{i=0}^{N-1} y_i - y_{(i+1)} \quad (4)$$

where y_i is the value of i -th sample; N is the total number of samples in the array. The mode evaluation coefficient k allows us to determine whether the strobe generator

frequency corresponds to the coherent sampling condition (2). In the case when the sampling mode approaches coherent, the samples of the harmonic reference clock are taken almost at the same points of the sinusoid, so the difference between the samples calculated by (3) decreases and the coefficient value becomes minimal. The example of dependence of the mode evaluation coefficient k on the sampling frequency when the reference clock frequency is equal to 10 GHz is shown in Fig.5.

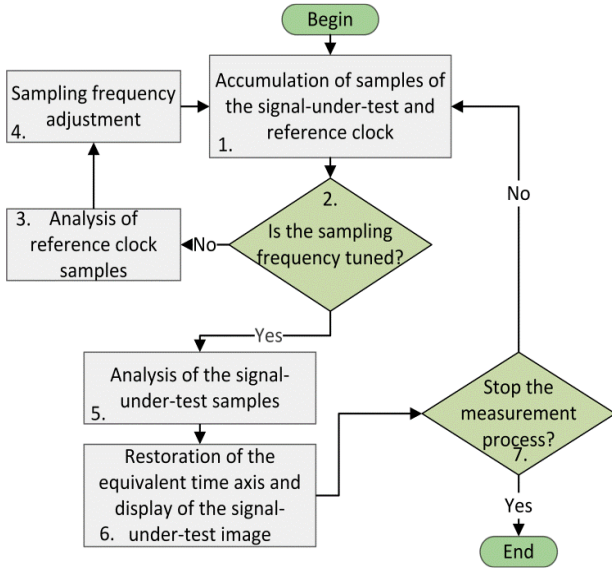


Fig.4. Flowchart for data processing and time-base device control.

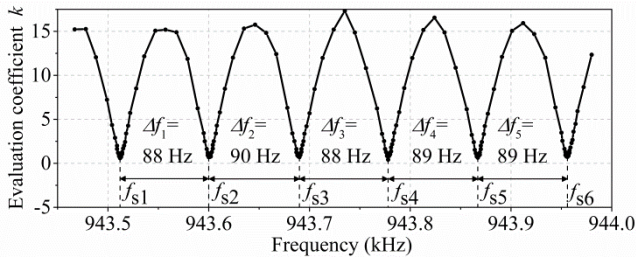


Fig.5. An example of dependence of the mode evaluation coefficient k on the sampling frequency when the reference clock frequency is equal to 10 GHz ($K = 6$).

b) From this dependence (Fig.5.), the frequency of the reference clock f_r is calculated by the following equation:

$$f_r = \frac{1}{K} \sum_{j=1}^{K-1} \frac{f_{s_j} \cdot f_{s_{(j+1)}}}{f_{s_{(j+1)}} - f_{s_j}}; \quad (5)$$

where f_{s_j} is the sampling frequency that is a multiple of the frequency of the reference clock, when the value of the coefficient k is minimal; K is the number of minimum points of the coherent sampling mode estimation coefficient (Fig.5.).

Step 4. In accordance with the frequency of the reference clock determined by (5), the optimal sampling frequency is matched, i.e., the goal is that between two “trigonometric” points there is a minimum amount of the “adjacent points”. To ensure that the number of samples n in one period of the reference clock will be optimum it can be determined by the relation:

$$n = \frac{T}{t_d} = \begin{cases} \frac{2\pi}{2 \cdot \cos^{-1} L} & \text{if } L > 0.707 \\ \frac{2\pi}{\pi - 2 \cdot \cos^{-1} L} & \text{if } L < 0.707 \end{cases}; \quad (6)$$

where $T = 1/f_r$ is the period of the harmonic reference clock; t_d is the duration of the shortest harmonic oscillation section, used to determine the time position of the sample according to one of the two techniques (Fig.6.), L is the switch-over level. For example, if the switch-over level corresponds to 0.707 of the amplitude of the harmonic oscillation, then $n = 4$.

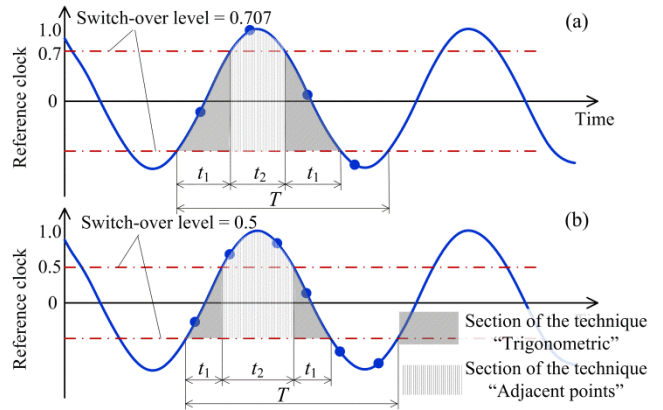


Fig.6. The relationship of the number of samples n per period of the reference clock and the magnitude of the switch-over level: a) level is equal to 0.707, $n = 4$; b) level is equal to 0.5, $n = 6$.

Step 5. At this stage, the algorithm returns to the main cycle (Steps 1, 2, 5–7). Sorting the samples of the harmonic reference clock is performed by assigning them to the equivalent-time axis restoration sections corresponding to the “trigonometric” or interpolation of “adjacent points” technique (Fig.7).

Step 6. At this stage, the algorithm returns to the main cycle (Steps 1, 2, 5–7). Sorting the samples of the harmonic reference clock is performed by assigning them to the equivalent-time axis restoration sections corresponding to the “trigonometric” or interpolation of “adjacent points” technique (Fig.7.).

Step 7. For each sample of the signal-under-test, a time position is calculated in the limit of one period of the reference clock. Next, the waveform of the signal-under-test is restored on the axis of equivalent-time, which is divided into 4 sections within one period of the reference clock (Fig.7.). In two sections (section 2 and section 4) the position of the sample of the signal-under-test on the axis of equivalent-time is determined by the

“trigonometric” technique and in the other two sections (section 1 and section 3) – by the interpolation of “adjacent points” technique. The jitter magnitude of the restored signal-under-test is different in different sections and depends on the frequency and amplitude of the reference clock (Fig.7.). In sections where the points are determined by the “trigonometric” technique jitter is smaller, so to reduce the jitter, the frequency of the reference clock is divided so that the ratio between the frequencies of the signal-under-test and the reference clock is 4. In this case, if the switching-over level between the techniques of determining the position of the sample on the time axis is 0.707, then the period of the test signal will be located in one section, the jitter in which there is a minimum.

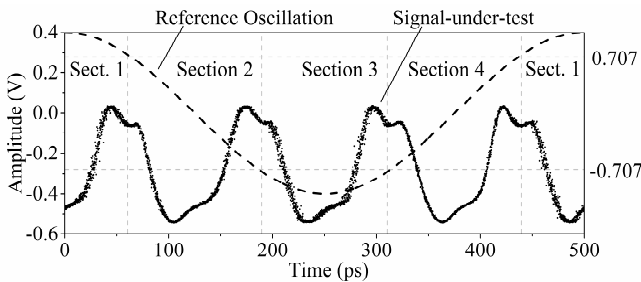


Fig.7. The example of restored waveform of the pulse signal in one period of the reference clock, when the switching-over level corresponds to 0.707 and the time axis is divided into 4 sections.

Step 8. The need for further measurement of the signal-under-test is checked at the last step of the main loop of the algorithm.

3. RESEARCH OF THE HYBRID TIME-BASE DEVICE

The experimental system was created to study the metrological characteristics of the proposed hybrid time-base device (Fig.8.). The prototype of the HTB device was implemented in a PicoScope-9301 sampling oscilloscope with a bandwidth of 25 GHz. VCO was introduced into the device and this provided the ability to adjust (to “scan”) the sampling frequency from 943 kHz to 947 kHz with 16-bit accuracy. Channel 1 of the oscilloscope was used to measure the signal-under-test, and channel 2 was used to measure the harmonic reference clock. The pseudo-random bit sequence (PRBS) generator Tektronix PPG1251, whose bit rate reaches 12.5 Gb/s, was used as the source of the signal-under-test. The output clocks of the PPG1251 are rectangular; therefore, harmonic oscillations were obtained using frequency divider UXN40M7K and Texas Instruments digitally-controlled variable-gain amplifier LMH6401 with a 4.5 GHz bandwidth that in this case also served as a low-pass filter. Discussing the hybrid base-time control algorithm, it was mentioned that the width of the time window, in which the restored signal-under-test is displayed on the axis of equivalent-time, depends on the value of the reference clock period and can be changeable (expandable) by dividing the reference clock frequency. Microsemi UXN40M7K frequency divider with a variable division ratio from 1 to 127 was used in the

experimental set-up, which made it possible to change the width of the time window from $1 \times 1/(12.5 \cdot 10^9 \text{ Hz}) \approx 80 \text{ ps}$ to $127 \times 1/(12.5 \times 10^9 \text{ Hz}) \approx 10.1 \text{ ns}$ when 12.5 GHz reference clock was used. The software for managing the HTB device was installed in the control computer connected to the oscilloscope via the USB interface.

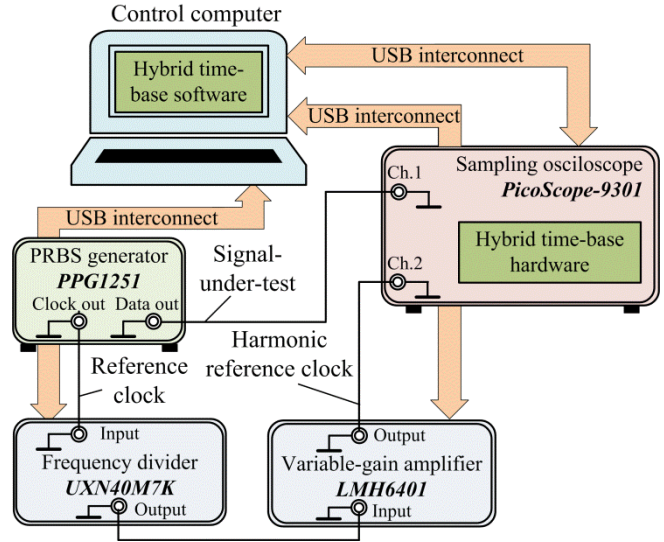


Fig.8. Organization of the experimental set-up.

The result of measuring the PRBS using the HTB device is shown in Fig.9. The bit rate in the PRBS was about 12.5 Gb/s, the highest jitter was observed at the center and edges of the “eye-diagram”, where the part of the sine wave of the reference clock was the most gentle and the position of the samples on the axis of equivalent-time was determined by the method of interpolation of “adjacent points”.

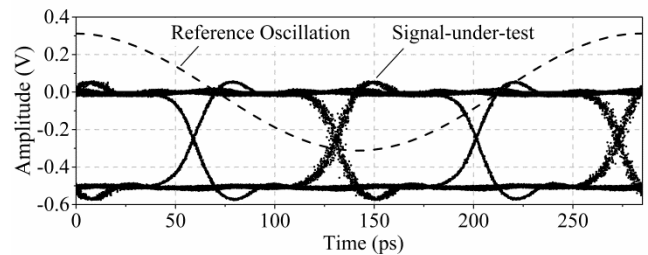


Fig.9. An image of the PRBS measured by the PicoScope-9301 oscilloscope using the hybrid time-base.

The functionality of the HTB device to select the period of the test signal with a minimum amount of jitter, where the position of the samples is determined by the “trigonometric” technique, is shown in Fig.10. The frequency division ratio of the UXN40M7K was set to four, i.e., one period of the reference clock corresponded to four periods of the signal-under-test. It can be seen here that by setting the switching-over level to 0.707, the minimum jitter equal to 700 fs, RMS was obtained. It is appropriate to note here that according to the specification of the PPG1251 when using the PRBS27-1 pattern, the jitter output data of the PPG1251 itself reaches 600 fs at a transmission rate of 12.5 Gb/s.

To determine how much jitter has the HTB device compared to a regular time-base device, the PRBS was measured with the same oscilloscope PicoScope 9301, but operating in the usual mode using its own sequential equivalent time-base device. The results of both measurements are presented in Fig.11. It is obvious that the jitter of the HTB device is two times less than the jitter of a sequential TB device.

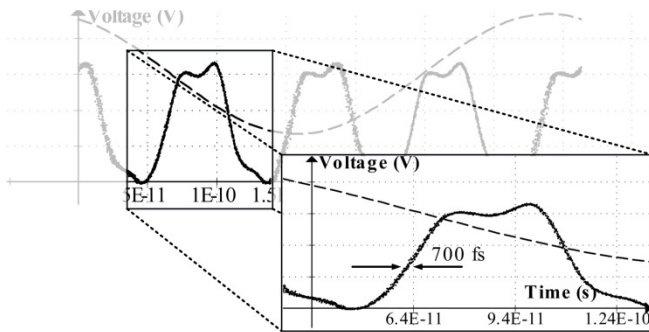


Fig.10. The selected bit of the measured PRBS with the least jitter.

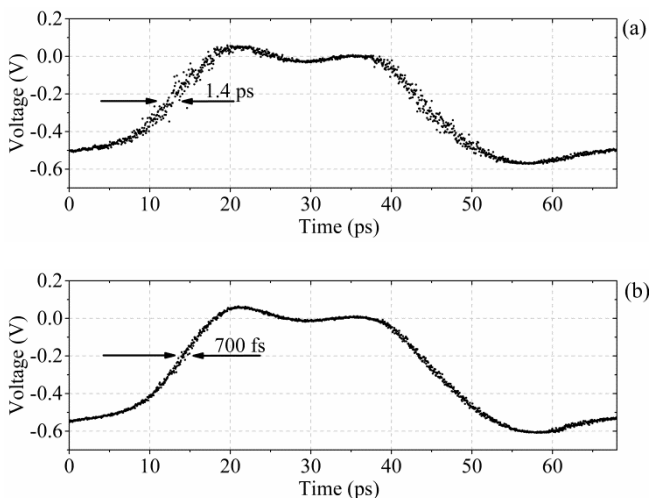


Fig.11. Comparison of maximum jitter: a) signal-under-test restored in the usual sequential time-base device; b) signal-under-test restored in the hybrid time-base device.

It is known that one of the significant components of the error in determining the position of the sample on the axis of equivalent time is the temperature drift. However, the feature of the HTB device is to use the reference clock from the system-under-test itself, which reduces temperature drift to a minimum. Of course, it completely depends on the temperature stability of the phase between the reference clock and the measured signal of the system-under-test. To demonstrate this feature, the 14 GHz harmonic waveform was measured continuously for one hour using the oscilloscope with a sequential equivalent TB device and the HTB device. The jitter distribution was accumulated for each TB device. The processed jitter distributions are shown in Fig.12.

It can be seen here (Fig.12.) that the jitter distribution of a sequential equivalent TB device for one hour is a displacement of 3.7 ps, and in the HTB device the distribution is normal, and its displacement is practically absent.

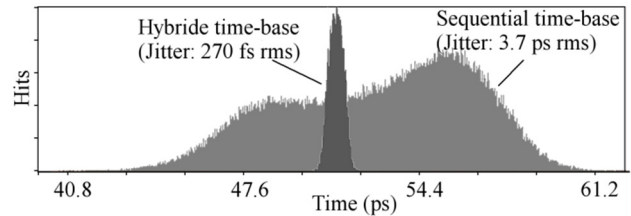


Fig.12. The drift of the distribution of jitter within one hour of the sequential base-time device and the hybrid base-time device.

4. CONCLUSIONS

A new technique to restore the equivalent time axis in modern sampling oscilloscopes, called the hybrid time-base (HTB) for the coherent sampling oscilloscope, is proposed in this paper. This technique of restoration of the time position of the samples is more accurate than the conventional time-base and has a smaller random error (jitter). In our case, coherent means that the frequency of the signal-under-test and the frequency of the strobe pulses are in a certain ratio. The idea of coherent sampling itself is well known, but in practice it effectively works only at sufficiently high frequency of the strobe pulses (usually dozens of megahertz) and at the frequency of the signal-under-test more than hundreds of megahertz. The main problem here is the long-term frequency stability of both the strobe pulses and the signal-under-test. In the proposed technique the coherent sampling mode is used to support optimal operation conditions for another way to restore the equivalent time-base, which we called "trigonometric". It should be noted that the proposed method can be implemented using only one additional sampling circuit, while similar solutions require a minimum of two sampling circuits and a phase shifter at 90 degrees.

It is known that the sampling oscilloscope operates more efficiently at low frequencies: the frequency of the strobe pulses is of the order of hundreds of kilohertz (at low frequency there is less noise of the vertical channel and wider bandwidth of the sampler). The prototype made by us demonstrated the possibility of functioning at a frequency of strobe pulses of 1 MHz and less.

Preliminary experimental studies of the proposed HTB device have shown that jitter can be reduced much more than 2.0 times. The experiment also showed that the drift component of the restoration error of the equivalent time axis is practically absent in the HTB device when signal-under-test and reference harmonic waveform are phase locked.

The most problematic in our study was the restoration of the time positions by the interpolation of "adjacent points" technique. In the future, to overcome this disadvantage, we will concentrate our research to ensure greater frequency stability of the coherent sampling mode.

Another disadvantage of the proposed HTB technique is that the determination of the temporal position of the sample directly depends on such metrological parameters of the

oscilloscope vertical channel as noise, temperature drift, and nonlinear distortion. Therefore, we intend to offer ways to reduce noise and nonlinearity of the vertical channel in the near future.

In addition to the above, the reference oscillation used in the HTB device should have low noise and not have extraneous harmonics. This is difficult to achieve in practice. Therefore, we intend to find a way to solve the problem of stringent requirements for the reference oscillation.

ACKNOWLEDGMENT

Many thanks to Mr. Jakovas Rososkis, the head of Company ELTESTA UAB, for fruitful discussions and moral support. For the actual analyses and experiments, infrastructure of the Company ELTESTA UAB was used.

REFERENCES

- [1] Pereira, J.M.D. (2006). The history and technology of oscilloscopes. An overview of its primary characteristics and working principles. *IEEE Instrumentation & Measurement Magazine*, 9 (6), 27-35.
- [2] Hale, P., Williams, D.F., Remley, K.A. (2007). The sampling oscilloscope as a microwave instrument. *IEEE Microwave Magazine*, 8 (4), 59-68.
- [3] Remley, K.A., Gordon, J.A., Novotny, D., et. al. (2017). Measurement challenges for 5G and beyond. *IEEE Microwave Magazine*, (18) 5, 41–56.
- [4] Avolio, G., Raffo, A., Jargon, J., Hale, P., Schreurs, D., Williams, D. (2015). Evaluation of uncertainty in temporal waveforms of microwave transistors. *IEEE Transactions on Microwave Theory and Techniques*, 63 (7), 2353–2363.
- [5] Tektronix, Inc. *Digital serial analyzer sampling oscilloscope DSA8300*. <https://www.tek.com/oscilloscope/dsa8300-sampling-oscilloscope>.
- [6] Keysight Technologies, Inc. *N1094A DCA-M sampling oscilloscope*. <https://www.keysight.com/en/pdx-2738546-pn-N1094A/dca-m-sampling-oscilloscope-two-electrical-channels?cc=LT&lc=eng>.
- [7] Clement, T.S., Hale, P., Williams, D.F., Wang, C.M., Dienstfrey, A., Keenan, D.A. (2006). Calibration of sampling oscilloscopes with high-speed photodiodes. *IEEE Transactions on Microwave Theory and Techniques*, 54 (8), 3173-3181.
- [8] Remley, K., Williams, D., Hale, P., Wang, C.-M., Jargon, J., Park, Y. (2015). Millimeter-wave modulated-signal and error-vector-magnitude measurement with uncertainty. *IEEE Transactions on Microwave Theory and Techniques*, 63 (5), 1710–1720.
- [9] Fuser, H., Eichstadt, S., Baaske, K., Elster, C., Kuhlmann, K., Judaschke, R., Pierz, K., Bieler, M. (2012). Optoelectronic time-domain characterization of a 100 GHz sampling oscilloscope. *Measurement Science and Technology*, 23 (2), 11 p.
- [10] Yuan, W., Jiangmiao, Z., Jingyuan, M. (2013). Correction of time base error for high speed sampling oscilloscope. In *IEEE 11th International Conference on Electronic Measurement & Instruments*, Harbin, China. IEEE, 88-91.
- [11] Wang, J.C.M., Hale, P.D., Jargon, J.A., Williams, D.F., Remley, K.A. (2012). Sequential estimation of timebase corrections for an arbitrarily long waveform. *IEEE Transactions on Instrumentation and Measurement*, 61 (10), 2689-2694.
- [12] Cirulis, R., Greitans, M., Hermanis, E. (2013). Time domain distortion estimation and correction using sample shifting procedure. *Elektronika ir elektrotechnika (Electronics and Electrical Engineering)*, 19 (9), 81-84.
- [13] Jargon, J.A., Hale, P.D., Wang, C.M. (2010). Correcting sampling oscilloscope timebase errors with a passively mode-locked laser phase locked to a microwave oscillator. *IEEE Transactions on Instrumentation and Measurement*, 59 (4), 916-922.
- [14] Boaventura, A., Williams, D., Avolio, G., Hale, P. (2018). Traceable characterization of broadband pulse waveforms suitable for cryogenic Josephson voltage applications. In *2018 IEEE/MTT-S International Microwave Symposium – IMS*, Philadelphia, USA. IEEE, 1176–1179.
- [15] Humphreys, D., Akmal, M. (2012). Channel timebase errors for Digital Sampling Oscilloscopes. In *2012 Conference on Precision electromagnetic Measurements*. IEEE, 2 p.
- [16] Cho, C., Lee, J., Hale, P., Jargon, J., Jeavons, P., Schlager, J., Dienstfrey, A. (2016). Calibration of time-interleaved errors in digital real-time oscilloscopes. *IEEE Transactions on Microwave Theory and Techniques*, 64 (11), 4071–4079.
- [17] Hale, P.D., Wang, C.M., Williams, D.F., Remley, K.A., Wepman, J. (2006) Compensation of a random and systematic timing errors in sampling oscilloscopes. *IEEE Transactions on Instrumentation and Measurement*, 55 (6), 2146-2154.
- [18] Hale, P.D., Dienstfrey, A., Wang, J.C.M., Williams, D.F., Lewandowski, A., Keenan, D.A., Clement, T.S. (2009). Traceable waveform calibration with a covariance-based uncertainty analysis. *IEEE Transactions on Instrumentation and Measurement*, 58 (10), 3554-3568.
- [19] Reader, H.C., Williams, D.F., Hale, P., Clement, T.S. (2008). Comb-generator characterization. *IEEE Transactions on Microwave Theory and Techniques*, 56 (2), 515-521.
- [20] Nelson, M. (2000). A new technique for low-jitter measurements using equivalent-time sampling oscilloscopes. In *56th ARFTG Conference Digest*, Boulder, USA. IEEE, 1-3.
- [21] IEEE. (2001). *IEEE Standard for Digitizing Waveform*.

Received January 23, 2019

Accepted May 30, 2019